Length Effect on Bending Properties and Evaluation of Shear Modulus of Parallel Bamboo Strand Lumber

Dong Yang[1,2], Haitao Li[1,2*], Dongdong Wei[3], Rodolfo Lorenzo[4], Ileana Corbi[5], Ottavia Corbi[5], Conggan Yuan[3], Zhenhua Xiong[6], Chaokun Hong[1,2], Huizhong Zhang[1,2]

[1a] College of Civil Engineering, Nanjing Forestry University, Nanjing 210037, China

[2] Joint International Research Laboratory for Bio-composite Building Materials and Structures, Nanjing Forestry University, Nanjing 210037, China

[3] Jiangxi Feiyu Bamboo Stock Co. LTD, Fengxin 330700, China

[4] University College London, London WC1E 6BT, UK.

[5] University of Naples Federico II, Via Claudio 21,80133 Naples, Italy.

[6] Ganzhou Sentai bamboo company LTD, Ganzhou 341001, China.

*Corresponding author: Haitao LI, Professor, E-mail: lhaitao1982@126.com

Abstract: 162 parallel bamboo strand lumber (PBSL) beams were tested for the bending properties under three-point bending with variable span. Two typical failure types were classified, type I was tension failure of the bamboo fiber located below the neutral axis at mid-span, while type II was shear failure which mainly found in specimens with large depth-span ratio. The shear modulus G_{LR} of PBSL was also calculated according to Timoshenko's bending theory. To evaluate the shear modulus, 45° off-axis compression tests had been done. The results showed that the mean values of shear modulus for G_{LT}, G_{TR}, and G_{LR} are 1254.5 MPa, 408.1 MPa, and 716.4 MPa respectively. The bending test result was compared with the shear modulus measured by 45° off-axis compression test. It was found that the shear modulus measured by three-point bending test with variable span was significantly less than the shear modulus obtained by 45° off-axis compression test. The empirical equation of shear factor s corresponding to depth-span ratio h/l was proposed. The calculation results gained from the proposed formula are in good agreement with the 45° off-axis compression test results.

Key words: parallel bamboo strand lumber (PBSL); three-point bending test; 45° off-axis test; shear modulus

1 Introduction

Due to the increasing shortage of wood resources and increasing human awareness of environmental protection, the idea of using bamboo as building material (Amada et al. 1997; Fei et al. 2019; Ghavami 2005; Okubo et al. 2004) has attracted more and more attention (Li et al. 2019a; Hong et al. 2019; Terai and Minami 2011; Verma and Chariar 2012) and several studies of raw bamboo have been conducted (Obataya et al. 2007; Richard 2013; Lorenzo and Mimendi 2020a, 2020b; Janssen 2012). To solve the problem of irregular shape, size limitation and low rigidity of raw bamboo, engineered bamboo products were developed (Li et al. 2019b; Mahdavi et al. 2012; Malanit et al. 2011; Chen et al. 2020) and parallel bamboo strand lumber (PBSL) is one of the products (Li et al. 2020; Wei et al. 2017).

Several researchers have studied the basic mechanical properties of PBSL. Li et al. (2019c, 2020) examined the influence of size and direction on compression performance and proposed the stress-strain relationship models for PBSL. Sharma et al. (2015a, b) studied the effect of processing method on the mechanical properties of PBSL. Li et al. (2015) examined the electrical measurement method to determine the elastic constants of PBSL. Xu et al. (2017) studied the effect of heat treatment or temperature on PBSL properties. Yu et al. (2017) investigated the preparation as well as physical, mechanical, and interfacial morphological properties of engineered PBSL. Ahmad and Kamke (2011) analyzed the physical and mechanical properties of PBSL made from Calcutta bamboo, and Kumar et al. (2016) investigated how density and water absorption influence the mechanical performance of PBSL. Nugroho et al. (2000, 2001) performed a research to determine the suitability of zephyr strand from moso bamboo for structural composite board manufacture. The performance of large-scale PBSL structural components was also investigated. Tan et al. (2020) studied the axial compression properties of the PBSL columns. Considering the influence of slenderness ratio and eccentricity, Li et al. (2015; 2019d) studied the eccentric compression performance of PBSL columns and some bearing capacity calculation formulas were proposed. Zhang et al. (2018) studied the bending properties of AFRP PBSL beams. Huang et al. (2015) examined the pure shearing parameters of PBSL in each main material plane and pointed out that shearing in transverse-to-grain plane presented the lowest shear modulus and strength.

For better application of PBSL in construction industry, the mechanical properties of PBSL have been studied with a range of test methods. However, except for rail shear method, other methods for determining the pure shear mechanical properties of PBSL parallel and perpendicular to grain have received little attention. There exist several methods (Aicher et al. 2016; Fellmoser and Blaß 2004; García et al. 2012; Haddou et al. 2017) that have been developed for timber or bamboo products to measure shear modulus such as 45° off-axis test, three-point bending test with variable span, free-plate torsion test (Wang et al. 2018) and so on. In an experiment applied to *Betula platyphylla Suk*, Wang et al. (2003) successfully measured the shear modulus by applying 45° off-axis compression test and variable span three-point bending test. Yoshihara et al. (1998, 2002, 2012) evaluated the shear modulus of different types of timber by static bending test, asymmetric four-point bending test and flexural vibration test, a modified formula for calculating the shear modulus of timber by static bending test was also proposed. Through a series of tests, Saliklis and Falk (2000) demonstrated the weakness of existing relationships correlating off-axis elasticity to shear modulus for wood composite panels and proposed a new relationship which performs better that existing equations.

As discussed above, study on the bending performance of PBSL is limited, especially considering the influence of the length. In addition, there are few studies on measuring the shear modulus of PBSL, which is one of the main mechanical parameters. Thus, a series of experiments were carried out on parallel bamboo strand lumber specimens in this paper. The results will be analyzed and employed to develop the necessary formula to approximate shear modulus of PBSL.

2 Experimental study

2.1 PBSL

Moso bamboo (*Phyllostachys pubescens*) harvested at the age of 3-4 years was selected to

produce the specimens. The upper part of the culms with a length of 2000 mm was cut and split into 20 mm wide strips. After the outer skin (epidermal) and inner cavity layer (pith peripheral) had been removed, the culms were split into bamboo filament bundles by a roller press crusher (Fig.1a), and then the filament bundles were dried and charred under the temperature of 165℃ and air pressure of 0.3 MPa. After this, the bundles were put into molds (Fig.1b) and pressed together with phenol glue by a transverse compression of 10.3 MPa under the temperature of 160℃ to manufacture PBSL specimens (Fig.1c). The process is shown in Fig.1. The final moisture content of PBSL was 8.22% and the density was 1250 kg/m^3.

(a) Bamboo strand bundles

(b) Molds for PBSL

(c) Hot pressing

(d) PBSL

(e) Cross-section for PBSL

Fig. 1 Main manufacturing process for PBSL (Li et al. 2019c)

2.2 Three-point bending test

2.2.1 Specimens

Ten groups of bending test specimens were designed with the same cross section of 50 mm × 50 mm. The number and span variation for each group are shown in Table 1 and the total number of bending specimens is 162. In Figure 2 the three main directions for the specimens are shown.

Table 1 Quantity of specimens of each span

Spans /mm	660	630	600	560	520	480	440	380	360	320
Quantity	16	16	16	16	16	16	16	16	22	12

Fig.2 Bending test for PBSL (L is longitudinal direction; R radial direction, and T the tangential direction).

2.2.2 Test method

According to ASTM D143-09 (2009), this paper adopted displacement-controlled loading,

and different initial loading speeds were used for specimens with different spans. To ensure complete failure of the specimens within 6-8 minutes, the loading speed was 10 mm/min after the first failure. The machine used in this test was a servo-controlled electro-hydraulic universal testing machine with a maximum load of 50 kN from SUNS stock, Shenzhen, China. The test scheme is shown in Fig.2.

Support marks were added to each specimen for placing the specimen accurately during the test. For each group, the span was modified accordingly. After the test, the failure type was recorded and the bending strength was calculated by Eq. (1),

$$\sigma = \frac{3P_{max}l}{2Ah} \tag{1}$$

where, σ is the bending strength, P_{max} is the ultimate load; l is the span of the beam; A is the cross-sectional area of the beam, h is the height of the beam.

2.2.3 Theory of measuring shear modulus by three-point bending test with variable span

The method of measuring shear modulus by three-point bending test with variable span is based on Timoshenko's beam theory, When the load P is imposed at center of the beam with a span of l, the mid-span deflection of the beam at elastic stage can be written as

$$w = w_m + w_s = \frac{Pl^3}{48EI} + \frac{sPl}{4GA} \tag{2}$$

where w is the total deflection of the beam; w_m is the deflection caused by bending moment; w_s is the deflection caused by shear force; P is the load imposed on the beam; E is the Young's modulus; G is the shear modulus; I is the moment of inertia; s is the shear factor which value is 1.2 according to ISO 8375:2009-02 (2009).

When the depth-span ratio h/l is small, the mid-span deflection can be directly represented by w_m in Eq.(2). When the depth-span ratio is large, the influence of shear force should be taken into account, that is, the deflection w_s caused by shear force in Eq. (2) cannot be ignored. Eq.(2) can be given as

$$w = \frac{Pl^3}{48I} \cdot \left(\frac{1}{E} + \frac{s}{G} \cdot \frac{h^2}{l^2} \right) = \frac{Pl^3}{48E_{app}I} \tag{3}$$

Then Eq.(3) could be obtained,

$$\frac{1}{E_{app}} = \frac{1}{E} + \frac{s}{G} \cdot \frac{h^2}{l^2} \tag{4}$$

where,E_{app} is the apparent modulus of elasticity, and its value can be obtained from the linear section of load P and mid-span deflection w relation. The values of E and G/s can be obtained by the relation between $1/E_{app}$ and the depth-span ratio h/l.

2.3 Compression test for elastic constants

2.3.1 Specimens

According to Chinese National Standard GB/T 15777-2017 (2017), specimens for compression test were extracted from the three-point bending test specimens. The position from which the samples were extracted is shown in Fig.3a. The size of the compression test specimen was 20 mm × 20 mm ×50 mm, and the number of the specimen was 12 for each direction.

2.3.2 Test method

The specimens were loaded axially with a loading speed of 0.2mm/min, and the attachment method of strain gauges is shown in Fig.3b. The strain gauges used in this paper were from Huangyan Linli Engineering Sensor Factory, Zhejiang, China, and the size was 10mm×3mm. The adhesive used for attachment was instantaneous drying glue 502 from Taizhou Henco-glue Co., Ltd, Zhejiang, China.

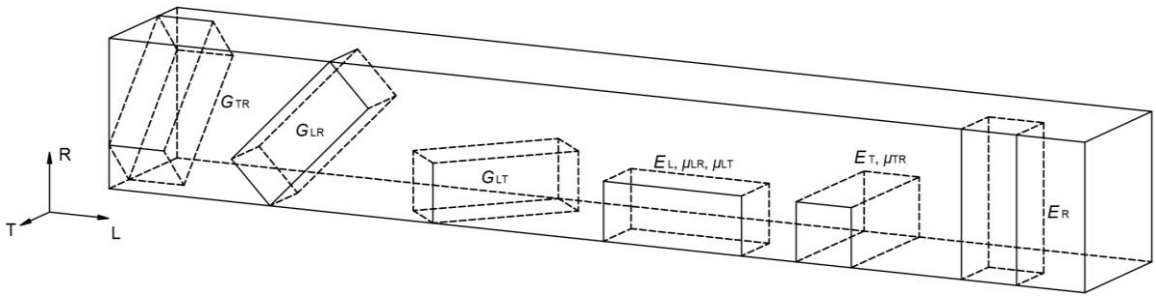

(a) Extracting method of specimens for compression test

(b) Attachment method of Strain gauges

Fig.3 Design of compression test. a) Extracting method of specimens for compression test, b) Attachment method of Strain gauges

Based on the test results, the Young's modulus E was calculated by Eq.(5):

$$E = \frac{\Delta P}{A\Delta\varepsilon} \tag{5}$$

where, E is the Young's modulus; ΔP is load increment; $\Delta\varepsilon$ is strain increment.

For off-axis compression test, there is an angle θ between the fiber direction and the compression direction; the shear force τ and shear strain γ could be obtained by Eq. (6-1) and Eq. (6-2):

$$\tau = \frac{\Delta P}{2A}\sin 2\theta \tag{6-1}$$

$$\gamma = \left(\varepsilon_x - \varepsilon_y\right)\sin 2\theta + \left(2\varepsilon_{45} - \varepsilon_x - \varepsilon_y\right)\cos 2\theta \tag{6-2}$$

where, $\varepsilon_x, \varepsilon_y, \varepsilon_{45}$ are the strain of the axial direction, transverse direction and 45degree direction of the test samples, respectively, as shown in Fig.3. Since θ is 45° for all the samples, the shear modulus was calculated by Eq. (7):

$$G^{45^\circ} = \frac{\tau}{\gamma} = \frac{\Delta P / 2A}{\varepsilon_x - \varepsilon_y} \tag{7}$$

where $G^{45°}$ is the shear modulus obtained by 45° off-axis compression test.

3 Test results and combined analysis

3.1 Failure phenomena of bending test

The load-deflection curves for different spans are shown in Fig.4. All specimens experienced first an elastic stage and then an elastic-plastic stage. No obvious failure phenomena on the surfaces could be seen for both elastic stage and elastic-plastic stage. However, with the increase in loading, two failure phenomena could be classified. The four sides of specimens were named as A, B, C, D (Fig.5) so that the description of the failure phenomena for each specimen could be done conveniently.

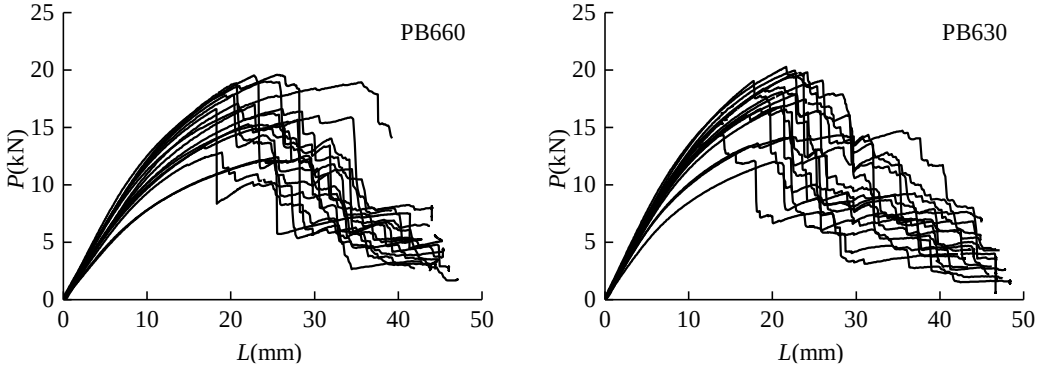

(a) PB660

(b) PB630

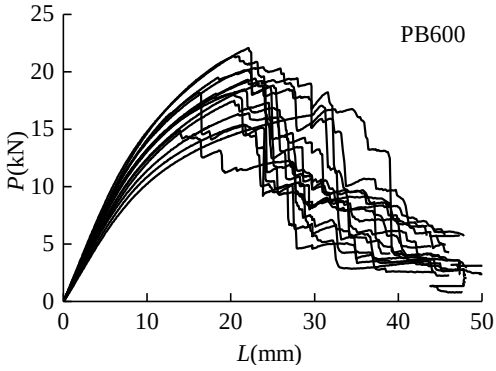

(c) PB600

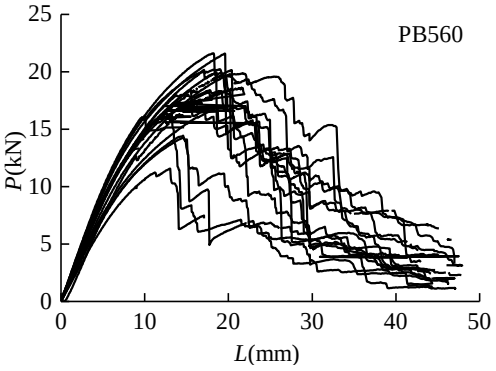

(d) PB560

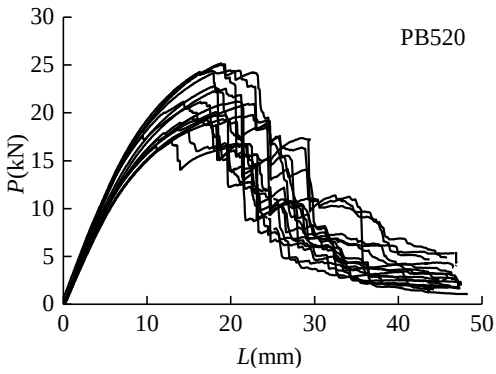

(e) PB520

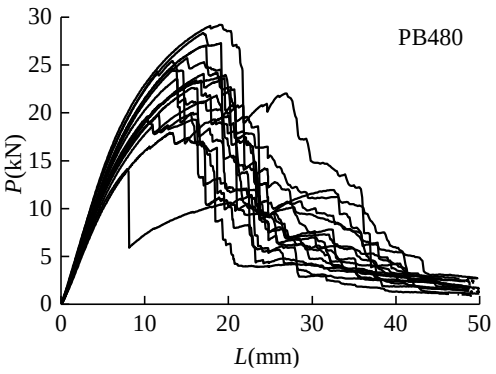

(f) PB480

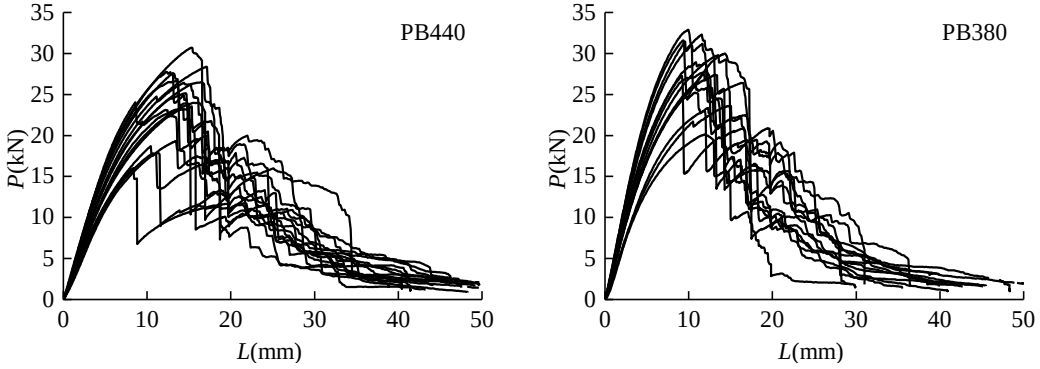

(g) PB440 (h) PB380

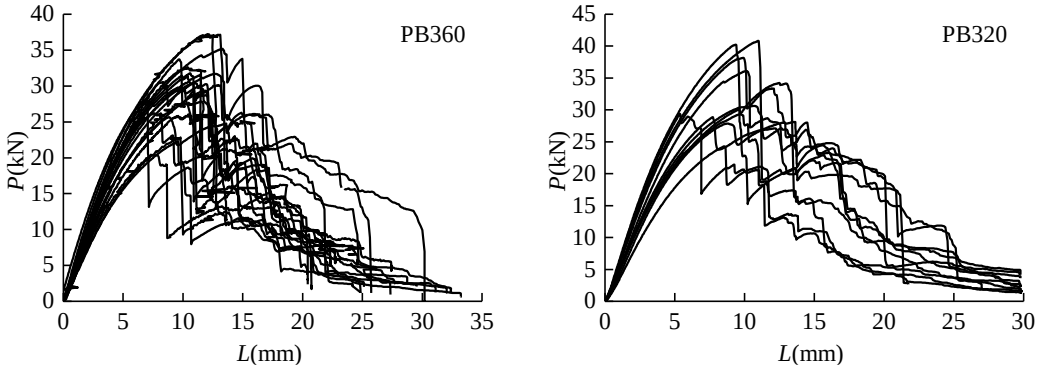

(i) PB360 (j) PB320

Fig.4 Load-deflection curves

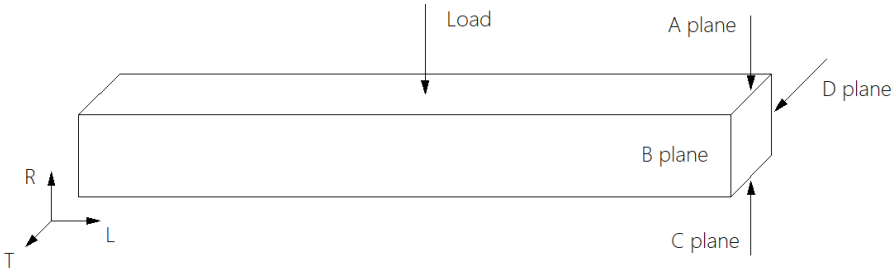

Fig.5 Naming of four sides of specimens

Failure type I, as shown in Fig.6a, was tension failure of the bamboo fiber at the middle and bottom of the span. When the ultimate load was reached, a sudden clear sound could be heard, a big crack appeared at the middle of C plane, and then transverse cracks appeared at D plane of the specimen. At this time, the fibers at the middle of C plane were pulled off while the unbroken fibers continued to bear the load. When the load was applied continuously, more cracks appeared in accordance with the same failure type, which was also the reason why the load-deflection curve (Fig.6c) of the specimens was ladder-shaped in the failure stage.

Failure type II was shear failure, as shown in Fig. 6b. With the increase in loading, transverse shear crack occurred suddenly along the L direction of the specimen, and a loud sound could be heard. At the same time, the load suddenly decreased, the specimen was destroyed into the upper and lower layers to continue bearing the load (Fig.6d).

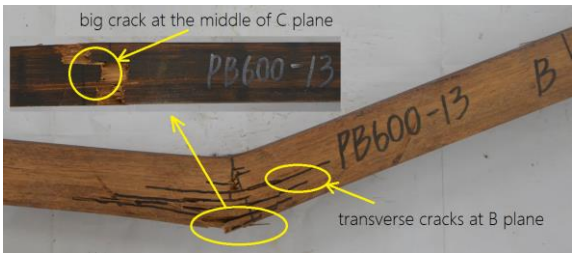

(a) Failure type I

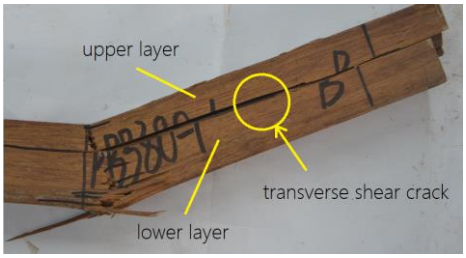

(b) Failure type II

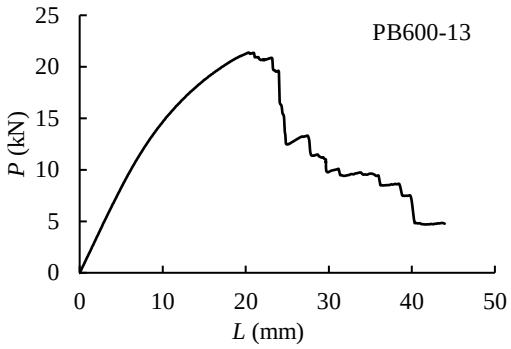

(c) PB600-13

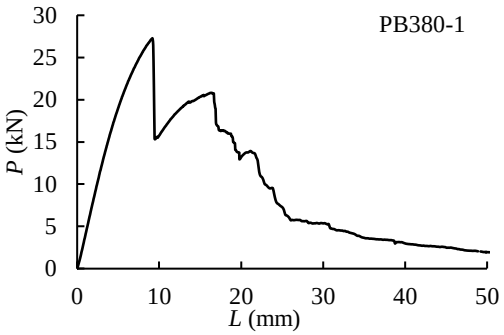

(d) PB380-1

Fig.6 Failure types (a,b) and typical load-deflection curves (c, d)

The percentage of failure type II for each span is shown in Table 2. When the span was greater than 480 mm (h/l<1), the failure type of the specimens was basically type I. However, the percentage of failure type II increased quickly with the decrease in the span when the span was less than 480mm (h/l>1). It reflected that when the depth-span ratio was large, the influence of shear force should not be ignored.

Table 2 Percentage of failure types for each span

Span /mm	660	630	600	560	520	480	440	380	360	320
Type I	16	16	15	15	14	13	15	4	6	3
Type II	0	0	1	1	2	3	11	10	16	9
Total	16	16	16	16	16	16	16	14	22	12
Percentage of type II	0%	0%	6.25%	6.25%	12.5%	18.5%	68.8%	71.4%	72.7%	75%

3.2 Test results for bending specimens

The test results for bending specimens are shown in Table 3. CHV means characteristic value, calculated on the basis that 95% of samples exceed the characteristic value (mean value - α × SDV, where α depends on the number of specimens). Figure 7 plots how the length values influence the bending properties of PBSL. For different spans, the bending strength σ had no significant variation with decreasing length. The mean value of σ for all the specimens was 108.93 MPa with a coefficient of variation of 13.65%. However, the mean value of apparent modulus of elasticity E_{app}^{b} decreased as the span decreased. Based on the test data, the following relationships could be obtained. Eq.(8-1) is the relationship between the ultimate bending strength and the depth-span ratio, Eq.(8-2) is the relationship between the apparent

modulus of elasticity E_{app}^{b} and the depth-span ratio. Combining Eq. (4) and Eq.(8-2), the shear modulus G_{LR}^{b} could be calculated, and the value was 284.33MPa.

$$\sigma = -200.31(h/l)^2 + 111.62 \tag{8-1}$$

$$1/E_{app}^{b} = 0.004221(h/l)^2 + 0.000062 \tag{8-2}$$

Table 3 Results of three-point bending test

Groups	σ				E_{app}^{b}			
	Mean /MPa	SDV /MPa	COV /%	CHV /MPa	Mean /MPa	SDV /MPa	COV /%	CHV /MPa
PB660	111.11	12.43	11.18	90.03	11324.66	1203.30	10.63	9283.86
PB630	110.37	15.38	11.73	84.29	11264.72	1320.82	11.73	9024.61
PB600	114.14	10.11	8.86	96.99	10626.92	944.29	8.89	9025.40
PB560	106.00	12.45	11.74	84.88	10443.1	1823.66	16.76	7350.17
PB520	112.21	12.52	11.16	90.98	9584.99	1279.41	13.35	7415.11
PB480	113.09	18.84	16.31	81.14	8769.96	929.61	10.60	7193.34
PB440	106.13	15.85	14.93	79.25	7920.93	807.81	10.20	6550.88
PB380	104.43	11.72	11.22	84.55	7194.1	908.01	13.42	5654.12
PB360	108.17	14.32	13.24	84.14	6935.79	727.91	10.49	5707.81
PB320	107.67	14.90	13.83	82.16	5639.06	694.29	12.31	4450.44

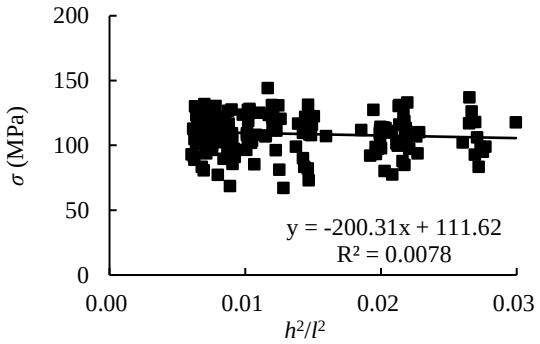

(a) Bending strength

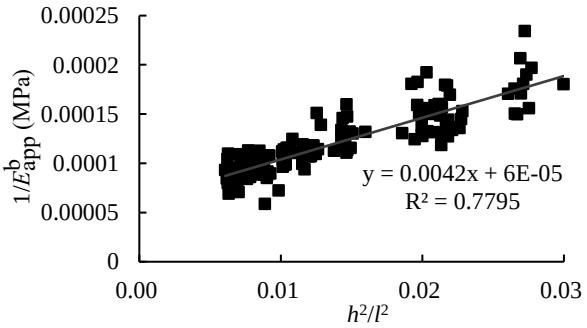

(b) Bending elastic modulus

Fig.7 Length effect on the bending strength (a) and bending elastic modulus (b)

3.3 Results of compression test

The results for 45° off-axis compression test are shown in Table 4. The mean values of shear

modulus f $G_{LT}^{45°}$, $G_{TR}^{45°}$, and $G_{LR}^{45°}$ are 1254.5 MPa, 408.1 MPa, and 716.4 MPa respectively. The mean values of Young's modulus E_L, E_T, E_R are 13752.4MPa, 2356.8MPa, 1052.9 MPa, respectively.

Table 4 Results of 45° off-axis compression test unit: MPa

Groups	$G_{LT}^{45°}$	Groups	$G_{TR}^{45°}$	Groups	$G_{LR}^{45°}$	Groups	E_L	Groups	E_T	Groups	E_R
G12-1	1195.36	G23-1	359.24	G13-1	716.76	E1-1	16016.8	E2-1	1506.01	E3-1	788.30
G12-2	1214.83	G23-2	439.23	G13-2	797.24	E1-2	11488.1	E2-2	980.24	E3-2	1314.76
G12-3	986.69	G23-3	405.60	G13-3	999.74	E1-3	13713.9	E2-3	1913.53	E3-3	712.30
G12-4	1239.05	G23-4	461.98	G13-4	846.48	E1-4	16734.4	E2-4	2982.97	E3-4	1331.50
G12-5	1229.37	G23-5	496.35	G13-5	691.57	E1-5	15224.9	E2-5	2031.25	E3-5	1062.96
G12-6	1291.36	G23-6	442.60	G13-6	534.50	E1-6	16913.9	E2-6	1743.53	E3-6	805.68
G12-7	1525.92	G23-7	434.63	G13-7	778.71	E1-7	11471.7	E2-7	2183.17	E3-7	1167.60
G12-8	1545.49	G23-8	544.53	G13-8	718.54	E1-8	10238.7	E2-8	3604.34	E3-8	1538.41
G12-9	1407.35	G23-9	562.82	G13-9	592.45	E1-9	-	E2-9	2689.29	E3-9	818.35
G12-10	1264.74	G23-10	-	G13-10	768.08	E1-10	17858.6	E2-10	1728.57	E3-10	774.32
G12-11	880.76	G23-11	549.15	G13-11	496.76	E1-11	10592.0	E2-11	2991.95	E3-11	902.14
G12-12	1273.46	G23-12	585.48	G13-12	655.43	E1-12	11024.8	E2-12	2547.89	E3-12	1418.60
Mean	1254.53	Mean	480.15	Mean	716.36	Mean	13752.4	Mean	2356.8	Mean	1052.91
SDV	182.77	SDV	69.26	SDV	132.70	SDV	2749.3	SDV	627.1	SDV	278.6
COV/%	14.57	COV/%	14.42	COV/%	18.53	COV/%	19.99	COV/%	26.61	COV/%	26.46

Based on Eq. (4) and the compression test results, the shear modulus obtained by two different methods is shown in Table 5.

Table 5 Shear modulus obtained by different methods.

Test methods	Three-point bending test with variable span (G_{LR}^{b})	45° off-axis compression test ($G_{LR}^{45°}$)
G / MPa	284.33	716.36

3.4 Discussion

The shear modulus measured by three-point bending with variable span method and 45° off-axis compression test was compared with the shear modulus of other bamboo and timber-based products in Table 6.

Table 6 Comparison of shear modulus

Authors	Test methods	Materials	Shearing plane	G/MPa
This paper	Three-point bending test with variable span	PBSL	G_{LR}	284
	45° off-axis compression test	PBSL	G_{LT}	1254
			G_{LR}	716
			G_{TR}	408
Li et al. (2015)	45° off-axis compression test	PBSL	G_{LT}	1347
			G_{LR}	823
			G_{TR}	567
Wang et al. (2003)	Three-point bending test with variable span	*Betula platyphylla Suk*	G_{LT}	609
			G_{LR}	971

Huang et al. (2015)	Rail shear test	PBSL	G_{LT}	1361
Yoshihara et al. (1998)	Flexural vibration test	Spruce	G_{LT}	910
		Western hemlock	G_{LT}	750
		Yellow poplar	G_{LT}	770

It can be seen from Table 5 and Table 6, that the shear modulus of PBSL obtained by 45° off-axis compression test in this paper was close to the results from Li et al. (2015) and was greater compared with other biomaterials. However, the shear modulus G_{LR}^{b} obtained by three-point bending test with variable span was obviously smaller than the shear modulus $G_{LR}^{45°}$ obtained by 45° off-axis compression test in this paper, which was similar to Yoshihara et al. (1998).

Figure 8a shows the relation between E_L^b/E_{app}^b-1 and h^2/l^2, where E_L^b was calculated by substituting the shear modulus $G_{LR}^{45°}$ measured by 45° off-axis compression test and the apparent elastic modulus E_{app}^b obtained by three-point bending test into Eq.(4). According to Timoshenko's theory, the relation should be linear and pass through the origin. In Fig. 8a, the relation between E_L^b/E_{app}^b-1 and h^2/l^2 showed a linear relation approximately when depth-span ratio h/l was less than 0.1, however, when h/l was greater than 0.1, the relation became discrete. Therefore, it could be concluded that for Timoshenko's beam theory to be valid, the depth-span ratio h/l should not be greater than 0.1. The percentage of failure type II for different spans also showed this trend. Figure 8b shows the relation between h^2/l^2 and the shear modulus $G_{LR}^{b'}$ obtained by substituting E_L in Table 4 and E_{app}^b from three-point bending test into Eq. (4). As one can observed, when the depth-span ratio h/l was less than 0.1, $G_{LR}^{b'}$ decreased as h^2/l^2 increased, the relation was approximately linear, and the linear relationship pointed to the true shear modulus, however, the shear modulus remained constant when h^2/l^2>0.1. According to Dong et al. (1994), the stress concentration near the loading point produced additional deflection. During the test, when h/l>0.1, the loading force was much bigger than that of h/l<0.1, meanwhile the elastic modulus E_R (1052.9 MPa, load direction) was the smallest, the influence of stress concentration was enlarged, this led to the test results were not reliable when h/l>0.1. So the value of G_{LR}^{b} when $h/l \leqslant 0.1$ was calculated and the value was 293.23MPa. Similar to Yoshihara et al. (1998), the shear modulus increased, but it was still very small. The physical evidence of stress concentration at loading point is shown in Fig.9. It is obvious that the deformation of 320mm-span specimen caused by the loading head was much greater than the deformation of 660mm-span specimen. In conclusion, it seems that the shear modulus cannot be calculated properly by three-point bending test with variable span.

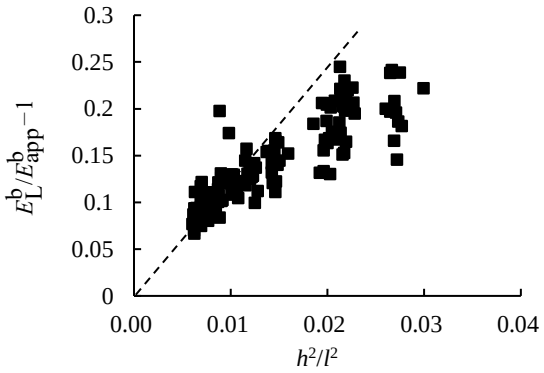

(a) (E_L^b/E_{app}^b-1)-h^2/l^2

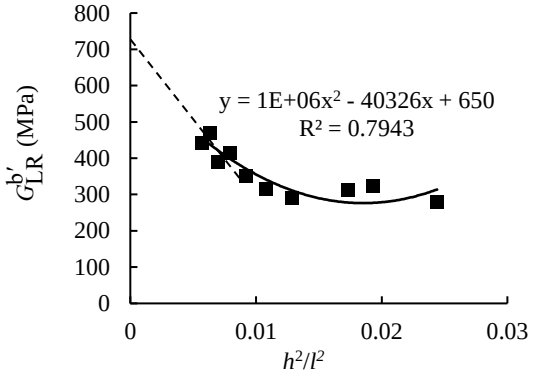

(b) $G_{LR}^{b'}$-h^2/l^2

Fig.8 Relationship among the parameters

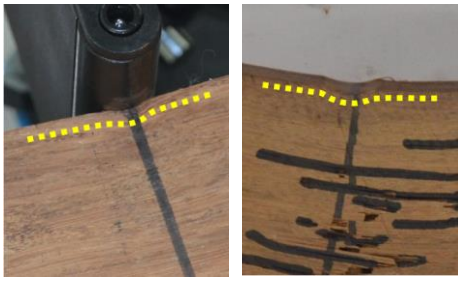

(a) Stress concentration when $h/l>0.1$ (PB320-2)

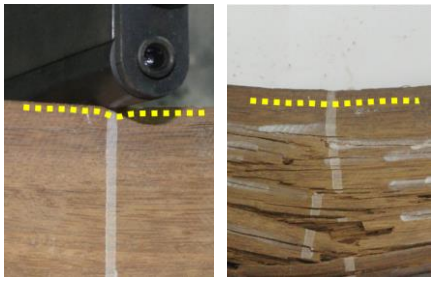

(b) Stress concentration when $h/l<0.1$ (PB660-5)

Fig.9 Stress concentration at the loading point, (a) $h/l>0.1$, (b) $h/l<0.1$

This paper attempted to modify the shear factor s in the original Timoshenko's theory so that the correct shear modulus can be obtained by three-point bending test with variable span.

According to Eq.(4), the shear factor s can be given as

$$s=\frac{G\left(\frac{1}{E_{app}}-\frac{1}{E}\right)}{\frac{h^2}{l^2}} \tag{9}$$

By substituting the shear modulus $G_{LR}^{45°}$ obtained by 45° off-axis compression test, E_L in Table 4 and E_{app}^{b} obtained by three-point bending test with variable span into Eq.(7), the relation between the shear factor s^b and the depth-span ratio h/l was obtained, as shown in Fig.10.

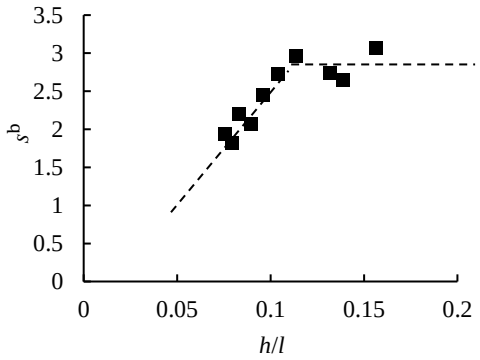

Fig.10 Relationship between the shear factor and the depth-span ratio

Therefore, the shear factor s could be given as s^* which related to the depth-span ratio h/l, as shown in Eq.(10),

$$s^*=k\frac{h}{l} \tag{10}$$

where k is a constant coefficient.

According to Fig. 9, the shear factor s^b was linear with depth-span ratio h/l at the beginning, while when the depth-span ratio was greater than 0.1, the shear factor s^b was a constant, which was 2.7.

Therefore, according to experimental test, the modified shear factor s^* could be expressed as Eq.(11),

$$s^*=\begin{cases} k\dfrac{h}{l} & \dfrac{h}{l}\le 0.1 \\ 2.7 & \dfrac{h}{l}>0.1 \end{cases} \tag{11}$$

where, k=2.7 according to test results.

Substituting the modified shear factor s^* in Eq.(10), E_L in Table 4, E_{app}^{b} obtained by three-point bending test into Eq.(4), the mean values of modified shear modulus G_{LR}^{b*} for different spans were calculated, as shown in Table 7. The mean value for G_{LR}^{b*} was 734.25 MPa with a coefficient of variation of 8.78%. The calculation results for the shear modulus from the proposed formula give better agreement with the test results from 45° off-axis compression test.

Table 7 Modified shear modulus G_{LR}^{b*}

Spans /mm	660	630	600	560	520	480	440	380	360	320
G_{LR}^{b*}/MPa	753.17	840.65	730.69	834.11	759.27	709.21	651.32	705.20	728.81	630.08

4 Conclusion

To evaluate the bending performance and the shear modulus of PBSL, both experimental study and numerical analysis were carried out.

Two typical failure types could be classified for PBSL beams under three-point bending test with variable span. Failure type Ⅰ was tension failure of the bamboo fiber at the middle and bottom of the span, while failure type Ⅱ was shear failure. Increment in the bending span did not have significant effect on bending strength, while the bending elastic modulus increased with the increment of bending span.

The calculation results for the shear modulus obtained by the three-point bending test were much smaller than that obtained by 45° off-axis compression test because the stress concentration near the loading point produced additional deflection. An empirical equation of shear factor s^* corresponding to depth-span ratio h/l was proposed which could be used for obtaining the shear modulus of PBSL.

Acknowledgments: The study is supported by the National Natural Science Foundation of China (51878354 & 51308301), the Natural Science Foundation of Jiang-su Province (No. BK20181402 & BK20130978), the China Postdoctoral Science Foundation (2015M580382), Jiangsu Postdoctoral Science Foundation Project (1501037A), Six Peak High-level Talents Project of Jiangsu Province, and a Project Funded by the Priority Academic Program Development of Jiangsu Higher Education Institutions. Any research results expressed in this paper are those of the writer(s) and do not necessarily reflect the views of the foundations. The authors gratefully acknowledge, Ke Zhou, Zhen Wang, Hang Li, Xiaoyan Zheng, Shaoyun Zhu, Liqing Liu, Dunben Sun, Jing Cao, Yanjun Liu and others from the Nanjing Forestry University for helping with the tests.

We declare that we do not have any commercial or associative interest that represents a conflict of interest in connection with the work submitted.

References

Ahmad M, Kamke FA (2011) Properties of parallel strand lumber from Calcutta bamboo (Dendrocalamus strictus). Wood Sci Technol 45(1):63-72

Aicher S, Christian Z, Hirsch M (2016) Rolling shear modulus and strength of beech wood laminations. Holzforschung, 70(8): 773-781

Amada S, Ichikawa Y, Munekata T, Nagase Y, Shimizu H (1997) Fiber texture and mechanical graded structure of bamboo. Compos Part B-Eng 28(1-2): 13-20.

ASTM D143-09 (2009) Standard test methods for small clear specimens of timber. ASTM International, West Conshohocken

Chen G, Yu Y, Li X et al (2020) Mechanical behavior of laminated bamboo lumber for structural application: an experimental investigation. Eur J Wood Prod 2020, 78(1):53-63

Divos F, Tanaka T, Nagao H, Kato H (1998) Determination of shear modulus on construction size timber. Wood Sci Technol 32(6):393-402

Dong Y, Nakao T, Tanaka C, Takahashi A, Nishino Y (1994) Effects of the shear, compression values of loading points, and bending speeds on Young's moduli in the bending of wood based panels. Mokuzai Gakkaishi 40:481-490

Fellmoser P, Blaß H J (2004) Influence of rolling shear modulus on strength and stiffness of structural bonded timber elements. CIB-W18 meeting (Vol. 37)

Fei B, Liu R, Liu X, X. Chen, S. Zhang (2019) A review of structure and characterization methods of bamboo pits. J For Eng 4(2):13-18

García J J, Rangel C, Ghavami K (2012) Experiments with rings to determine the anisotropic elastic constants of bamboo. Constr Build Mater 31: 52-57

GB/T 15777-2017 (2017) Method for determination of the modulus of elasticity in compression parallel to grain of wood. China Standard Press, Beijing

Ghavami K (2005) Bamboo as reinforcement in structural concrete elements. Cement Concrete Compos, 27(6): 637-649

Haddou G, Dandurand J, Dantras E, Maiduc H, Thai H, Giang N V, Lacabanne C (2017) Physical structure and mechanical properties of polyamide/bamboo composites. J Therm Anal Calorim 129(3): 1463-1469

Hong C, Li H, Lorenzo R, Wu G, Corbi I, Corbi O, Xiong Z, Yang D, and Zhang H (2019) Review on connections for original bamboo structures. J Renew Mater 7(8): 713-730

Huang D, Bian Y, Zhou A, Sheng B (2015) Experimental study on stress–strain relationships and failure mechanisms of parallel strand bamboo made from phyllostachys. Constr Build Mater 77: 130-138

ISO 8375:2009-02 (2009) Timber structures - Glued laminated timber - Test methods for determination of physical and mechanical properties. International Organization for Standardization

Janssen J J (2012) Mechanical properties of bamboo (Vol. 37). Springer Science & Business Media

Kumar A, Vlach T, Laiblova L, Hrouda M, Kasal B, Tywoniak J, Hajek P (2016) Engineered bamboo scrimber: Influence of density on the mechanical and water absorption properties. Constr Build Mater 127:815-827

Li H, Wu G, Xiong Z et al (2019a) Length and orientation direction effect on static bending properties of laminated Moso bamboo. Eur J Wood Prod 77(4):547-557

Li H, Liu R, Lorenzo R, Wu G, Wang L (2019b) Eccentric compression properties of laminated bamboo lumber columns with different slenderness ratios. Proc Inst Civil Eng Struct Build 172(5):315-326

Li H, Qiu Z, Wu G, Wei D, Lorenzo R, Yuan C, Zhang H, Liu R (2019c) Compression behaviors of parallel bamboo strand lumber under static loading. J Renew Mater 7(7):583-600

Li H, Qiu Z, Wu G et al (2019d) Slenderness ratio effect on eccentric compression performance of parallel strand bamboo lumber columns. J Struc Eng 145(8):04019077

Li H, Su J, Deeks AJ, Zhang Q, Wei D, Yuan C (2015) Eccentric compression performance of parallel bamboo strand lumber columns. BioResources 10(4):7065-7080

Li H, Zhang H, Qiu Z, Su J, Wei D, Lorenzo R, Yuan C, Liu H, and Zhou C (2020) Mechanical properties and stress strain relationship models for bamboo scrimber. J Renew Mater 8(1): 13-27

Li X, Xu M, Cai Y, Ren H, Zhong Y (2015) Determination of elastic constants of recombinant bamboo for structural material using an electrical measurement method. J Anhui Agric Univ 42(5):756-760

Lorenzo R, Mimendi L (2020a) Digitisation of bamboo culms for structural applications. J Build Eng 29: 101193

Lorenzo R, Mimendi L, Godina M, Li H (2020b). Digital analysis of the geometric variability of Guadua, Moso and Oldhamii bamboo. Constr Build Mater 236: 117535

Mahdavi M, Clouston P L, Arwade S R (2012). A low-technology approach toward fabrication of laminated bamboo lumber. Constr Build Mater 29: 257-262

Malanit P, Barbu M C, Frühwald A (2011) Physical and mechanical properties of oriented strand lumber made from

an Asian bamboo (Dendrocalamus asper Backer). Eur J Wood Prod 69(1): 27-36

Nugroho N, Ando N (2000) Development of structural composite products made from bamboo I: fundamental properties of bamboo zephyr board. J Wood Sci 46(1): 68-74

Nugroho N, Ando N (2001) Development of structural composite products made from bamboo II: fundamental properties of laminated bamboo lumber. J Wood Sci, 47(3): 237-242

Obataya E, Kitin P, Yamauchi H (2007). Bending characteristics of bamboo (Phyllostachys pubescens) with respect to its fiber–foam composite structure. Wood Sci Technol 41(5): 385-400

Okubo K, Fujii T, Yamamoto Y (2004). Development of bamboo-based polymer composites and their mechanical properties. Compos Part A-Appl Sci Manuf 35(3): 377-383

Richard M J. (2013). Assessing the performance of bamboo structural components. Dissertation, University of Pittsburgh

Saliklis E P, Falk R H (2000) Correlating off-axis tension tests to shear modulus of wood-based panels. J Struct Eng 126(5): 621-625

Sharma B, Gatóo A, Bock M, Ramage M (2015a) Engineered bamboo for structural applications. Constr Build Mater 81:66-73

Sharma B, Gatóo A, Ramage MH (2015b) Effect of processing methods on the mechanical properties of engineered bamboo. Constr Build Mater 83:95-101

Tan C, Li H, Wei D, Lorenzo R, Yuan C (2020) Mechanical Performance of Parallel Bamboo Strand Lumber Columns under Axial Compression: Experimental and Numerical Investigation. Constr Build Mater 231: 117168

Terai M, Minami K (2011) Fracture behavior and mechanical properties of bamboo reinforced concrete members. Proced Eng 10: 2967-2972

Verma C S, Chariar V M (2012) Development of layered laminate bamboo composite and their mechanical properties. Compos Part B-Eng 43(3): 1063-1069

Wang L, Lu Z, Shen S (2003) Study on twelve elastic constant values of Betula platyphylla Suk. J Beijing For Univ 25(6):64-67

Wang Z, Wang Y, Cao Y, Gao Z (2018) Measurements of the shear modulus of materials by the free-plate torsional mode shape method. J Test Evaluation 47(2):1163-1181

Wei Y, Ji X, Duan M, Li G (2017) Flexural performance of bamboo scrimber beams strengthened with fiber-reinforced polymer. Constr Build Mater 142(7): 66-82.

Xu M, Cui Z, Chen Z, Xiang J (2017) Experimental study on compressive and tensile properties of a bamboo scrimber at elevated temperatures. Constr Build Mater 151:732-741

Yoshihara H, Kubojima Y, Nagaoka K, Ohta M (1998) Measurement of the shear modulus of wood by static bending tests. J Wood Sci 44(1):15-20

Yoshihara H, Kubojima Y (2002) Measurement of the shear modulus of wood by asymmetric four-point bending tests. J Wood Sci 48(1): 14-19

Yoshihara H (2012) Off-axis Young's modulus and off-axis shear modulus of wood measured by flexural vibration tests. Holzforschung, 66(2): 207-213

Yu Y, Liu R, Huang Y, Meng F, Yu W (2017) Preparation, physical, mechanical, and interfacial morphological properties of engineered bamboo scrimber. Constr Build Mater 157:1032-1039

Zhang H, Li H,Corbi I, Corbi O,Wu G,Zhao C, Cao T (2018) AFRP influence on parallel bamboo strand lumber beams. Sensors, 18(9):2854